What Proportion of the North Pacific Current Finds its Way into the Gulf of Alaska?

Howard J. Freeland*

DFO Science, Pacific Region
Institute of Ocean Sciences
P. O. Box 6000, Sidney BC V8L 4B2

ABSTRACT   *This paper builds on methods previously developed to show how the absolute geostrophic circulation of the Gulf of Alaska can be observed. A time series of maps of the monthly circulation patterns in the Gulf allows us to determine how much water is carried from the North Pacific Current and thence into either the Gulf of Alaska or the California Current System. This is of interest because of previous suggestions that fluctuations in the Alaska Current and the California Current might be anti-correlated. I will show that roughly 60% of the water arriving off the west coast of the Americas in the North Pacific Current eventually flows into the Gulf of Alaska, the remaining 40% flowing into the California gyre. Fluctuations in the North Pacific Current do occur, but the dominant response is a simultaneous strengthening of both the Alaska and California Currents. A significantly smaller fraction of variance in the North Pacific Current flow results in a change in the fraction of water supplied to either gyre.*

RÉSUMÉ   *[Traduit par la rédaction] Cet article s'appuie sur des méthodes précédemment mises au point pour montrer comment la circulation géostrophique absolue du golfe d'Alaska peut être observée. Une série chronologique de cartes des configurations de circulation mensuelles dans le golfe permet de déterminer quelle quantité d'eau est transportée à partir du courant du Pacifique Nord soit dans le golfe d'Alaska soit dans le système du courant de Californie. Ceci présente un intérêt en raison des suggestions précédentes à l'effet que les fluctuations dans le courant d'Alaska et le courant de Californie pourraient être anti-corrélées. Je vais montrer qu'environ 60 % de l'eau qui arrive par la côte ouest des Amériques dans le courant du Pacifique Nord finit par circuler dans le golfe d'Alaska, le reste (40 %) allant s'intégrer à la circulation de Californie. Il se produit des fluctuations dans le courant du Pacifique Nord, mais la réponse principale est un renforcement simultané des courants de l'Alaska et de Californie. Une fraction nettement plus petite de variance dans l'écoulement du courant du Pacifique Nord produit un changement dans la fraction d'eau fournie à l'une ou l'autre des circulations.*

1 Introduction

The circulation in the Gulf of Alaska (see Fig. 1) is dominated by the eastward flowing North Pacific Current (NPC) which bifurcates near the latitude of Vancouver Island with a north-flowing branch forming the Alaska Current, and a south-flowing branch forming the California Current. The Alaska Current is renamed the Alaska Stream after it rounds the northern Gulf of Alaska and becomes a narrow western boundary current.

There is a long-standing interest in determining the fraction of water arriving off the west coast of North America in the North Pacific Current that eventually flows into either the Alaska Current or the California Current. Assuming that water transports are conservative, then it is evident that $T_{NPC} = T_{GAk} + T_{CCurr}$, where T_{NPC}, T_{GAk} and T_{CCurr} represent transports in the North Pacific Current, the Gulf of Alaska and

the California Current respectively. (The abbreviations NPC, GAk and CCurr will be used in the remainder of this paper.) This raises the interesting possibility that variability in the total transport could be relatively small, but if the location of the bifurcation point changes substantially then we might observe large fluctuations in the GAk and CCurr that are negatively correlated with each other. The earliest reference to this phenomenon appears to be by Doe (1955) who examined dynamic topography in the GAk and concluded that the latitudes of the bifurcation of the NPC differed between 1950 and 1951. Wickett (1966) also examined the variability in the bifurcation and appears to be the first person to recognize that such variations could have biological effects.

This possibility was explored again by Chelton and Davis (1982) who looked at co-variability in sea levels along the

---

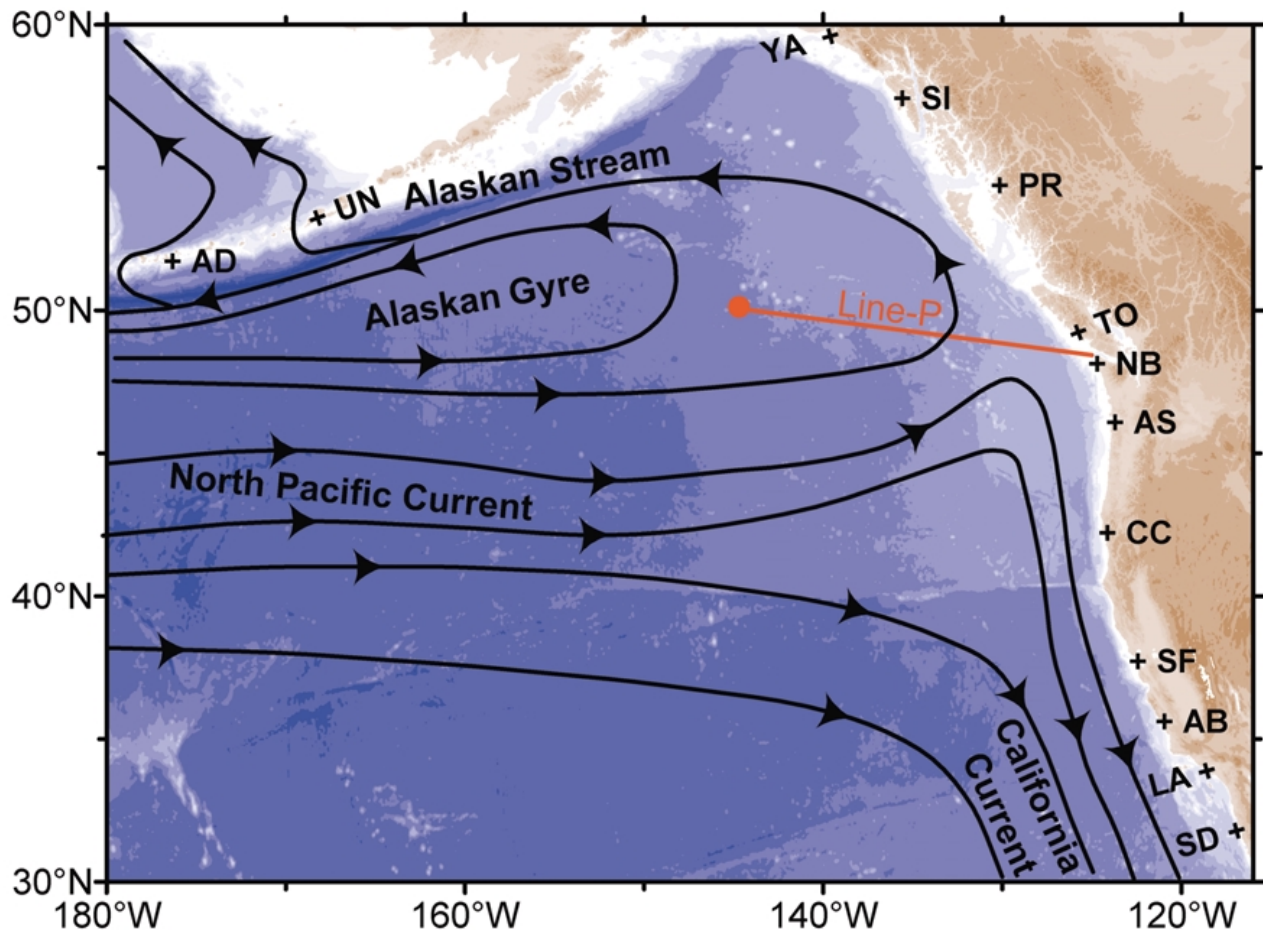*Author's e-mail: FreelandHj@pac.dfo-mpo.gc.ca

Fig. 1   A schematic presentation of the background flow in the GAk (based on Dodimead et al., 1963). Also indicated are the locations of Line-P and Ocean Station Papa. The area covered by this map will be used in later maps of the observed circulation. The letters and + symbols indicate sea-level observation sites that will be referred to in other parts of the paper.

Pacific coasts of the Americas. They identified a dominant mode of low frequency sea-level variability that could be explained by negative correlation of transports in the CCurr and GAk, like Wickett they suggested that such shifts could easily have significant impacts on the ecosystems of the two current systems. Francis and Sibley (1991) noted an apparent climate-related inverse decadal-scale relationship between the abundances of Alaska pink and West Coast coho salmon. Hare et al. (1999) examined correlated responses among time series of salmon return and various physical time series and reported "inverse production regimes". If this is correct then it suggests a powerful means of relating changes in the circulation of the GAk to biological systems.

Support for this concept might be gleaned from the various reports on the unusual conditions in the GAk during 2002 and early 2003 (Freeland et al., 2003; Kosro, 2003; Strub and James, 2003; Bograd and Lynn, 2003). These unusual conditions likely were forced by large-scale changes in the wind patterns (Murphree et al., 2003) and were accompanied by elevated nutrient concentrations in regions close to the coast (Wheeler et al., 2003) and increased primary production (Wheeler et al., 2003; Thomas et al., 2003). The paper by

Bograd and Lynn (2003) in particular suggested that there was a southward shift of the NPC bifurcation during 2002, however, detailed analysis by Freeland and Cummins (2005) (hereinafter FC) disproved this possibility. Additionally, several of the papers referred to above reported increases in the southward transport of the CCurr which were verified by FC.

An alternate, mode of variation would have the bifurcation essentially fixed so that fluctuations in T_{NPC} are manifested by responses in T_{GAk} and T_{CCurr} that are correlated with T_{NPC}, and therefore with each other.

This paper uses the Argo array in the GAk to explore the general circulation of the region. The Argo array is being deployed by a large international consortium and is more than adequately described elsewhere, such as FC.

In this paper I will describe methods that extend the mapping processes developed by FC to allow the description of the general circulation of the GAk. The barotropic corrections will be shown to be very small and negligible. I will then develop time series of the difference in dynamic height across the NPC, GAk and CCurr and explore the relationships among these variables.

2 The absolute circulation of the North-East Pacific

FC demonstrated a simple and efficient method for representing the geostrophic circulation in an ocean basin by projecting computations of dynamic height, relative to a level of no motion, onto empirical orthogonal functions of the streamfunction field. The streamfunction field is derived from a quasi-geostrophic model of the north-east Pacific described in Cummins and Lagerloef (2004). The method is quite straightforward and all computations can be performed on a small computer.

1) At the site of every Argo float profile in a particular month, the dynamic height at the surface is computed relative to a reference level, usually 1000 dbars.
2) The mean value is computed and subtracted from the observations to produce the first set of residuals. The mean-square value of these residuals is the variance to be accounted for.
3) The best fit between the residuals and the first empirical orthogonal function (EOF) is computed and the loading of the first EOF is stored. This weighted EOF is then subtracted from the residuals to produce a set of residuals with a smaller variance.
4) The best fit between the new residuals and the second EOF is computed, this mode is now subtracted from the residuals, and so on for a total of 20 EOFs.

At first, it seems unnecessary to subtract each of the modes in turn before proceeding to the best fit of the next mode, after all, the EOFs by definition are orthogonal. So, why is this operation carried out? Indeed, in the continuous sense, the streamfunction EOFs are orthogonal in the sense that for a set $\{\psi_n\}$, where in this case n runs from 1 to 20, then it can certainly be verified that:

$$\iint \psi_n(x, y)\psi_m(x, y)\, dx\, dy = \delta_{nm}$$

therefore, no two modes can interact with each other. However, the floats are not distributed evenly over the GAk and a more appropriate measure of orthogonality can be defined for the case where the modes ψ_n are observed at the locations (x_i, y_i) of floats, where i runs from 1 to N:

$$\sum_{i=1}^{N} \psi_n(x_i, y_i)\psi_m(x_i, y_i) = C_{nm}$$

and the correlation matrix C_{nm} would be precisely diagonal if the streamfunction modes were exactly orthogonal in the frame of reference of the float sampling. In this case it is only a diagonal-dominant matrix, meaning that the cross correlations ($n \neq m$) are much smaller than the auto-correlations ($n = m$). For one recent case, mapping dynamic heights in the north-east Pacific for June 2005 we find the rms value of $C_{n \neq m}$ is 0.14 with $N = 266$. Thus there is the possibility that the same contributions to the total variance will be accounted for by two or more different modes. This can lead to the implausible result of the process accounting for more than 100% of the target variance. More typically, as outlined in FC, this process accounts for between 85% and 90% of the variance, and in a few rare cases can account for up to 95%. The result is a set of maps that fit the observations of dynamic height, and satisfy the boundary conditions of zero flow through continental boundaries. This process also allows the estimation of flow in narrow boundary layers that are not resolved in the Argo array. Since each EOF is derived from an internally consistent model of the north-east Pacific, broad flows may be mapped that feed into a western continental boundary thus implying the existence of a western boundary current. Thus the maps presented in FC do show the presence of the Alaska Stream, and this is consistent with the Argo profiles.

Argo floats supply excellent quality profiles of temperature and salinity, but they also supply deep drift segments that allow estimates of the deep velocity field. Therefore, it should be possible to examine the distribution of velocities at the reference level and so compute a pressure field at that level. Added to the geostrophic circulation field this will yield a surface circulation field relative to a level of *known* motion. This field is estimated in very much the same way as the EOF fits to the dynamic height estimates. The result is that the observed surface circulation includes both the barotropic and baroclinic fields.

From the set $\{\psi_n\}$ we compute two new sets of functions $\{U_n\}$ and $\{V_n\}$ where:

$$U_n = -\frac{\partial \psi_n}{\partial y} \text{ and } V_n = \frac{\partial \psi_n}{\partial x}.$$

These new sets of modes are, in general, not orthogonal though they do tend to be predominantly so. Experiments with the set of streamfunction modes used in these computations shows that the sets $\{U_n\}$ and $\{V_n\}$ have off diagonal elements (after normalizing all diagonal elements to unity) with rms values of about 0.15.

To estimate the deep circulation field we first compute deep velocities as seen at Argo floats for a given month. Individual velocity estimates tend to be fairly noisy, and are computed by taking the last satellite position before a float dives and considering that to be the start position of a deep-drift phase. The next important position is that first acquired when a float appears at the surface 10 days later. Errors appear in several ways:

1) Service Argos supplies positions that can be within ± 150 m, but sometimes are only within ± 500 m. This error is random and can be reduced by averaging over several drift intervals.
2) There is a time delay between the arrival of a float at the sea surface and its acquisition by a satellite, and a delay between the last signal received by a satellite and the actual dive time of the float. These time intervals are not known and represent small but systematic errors. The

actual time between disappearance from the sea surface and arrival back at the surface 10 days later is always shorter than that observed. The Argos satellites are all in polar orbits and so the time delays in most of the GAk are probably quite short, of the order of 10 to 20 minutes. It probably is not worth the large effort required to make these small corrections

3) The 10-day displacement is contaminated by unknown drift as the float moves through higher velocity regions during ascent towards the sea surface. It is likely that this might be estimated if we are able to run, at some stage, an ocean data assimilation model. The contamination might be estimated through some kind of feedback from the model. At the moment this is not available. This error is most likely neither entirely random nor entirely systematic, rather it will depend on the strength of the near-surface flow.

In order to minimize especially the effect of error type 1, I chose to look at the Argo deep displacements over a three-month interval. Thus, for a particular float, deep drifts are estimated for a central month and for the months immediately before and afterwards. The average deep drift velocity is then computed and assigned a position appropriate to the centre of the central month.

Assume that resulting from the above we have N estimates of velocity (u_i, v_i) at locations (x_i, y_i) where the index i runs from 1 to N. We then find the weight w_j of the velocity modes (U_j, V_j) such that an error norm ε_j (mean-square error for mode j) is minimized where:

$$\varepsilon_j = \sum_{i=1}^{N}\left[\left(u_i - w_j U_j\left(x_i, y_i\right)\right)^2 + \left(v_i - w_j V_j\left(x_i, y_i\right)\right)^2\right].$$

The deep streamfunction field can then be estimated as a sum of the $\{\psi_j\}$ modes which, with appropriate scaling, becomes the deep pressure field through the geostrophic relation. When this deep pressure field is added to the surface geostrophic pressure field the result is the absolute dynamic height at the surface relative to a level of known motion, the depth at which Argo floats drift. Inevitably the deep pressure fit is noisier than the fit to the surface dynamic heights. Typically this fit accounts for only about 50% to 60% of the variance.

Figure 2 shows two plots, the left panel is the dynamic height at the sea surface relative to a level of no motion and the right panel shows the corrected dynamic height found by adding the pressure at the reference level. The circulation at the deep reference level is not shown, because the dynamic range is so small. It is apparent here that the two diagrams, Fig. 2a and Fig. 2b, are virtually indistinguishable. Other months have been examined, and in no month does the deep pressure correction result in a significant change to the pattern of circulation at the surface. In all that follows, the deep pressure correction will, therefore, be ignored.

3 Variability in the bifurcation of the North Pacific Current

Though in all subsequent analysis we will examine monthly circulation fields, Fig. 3 shows the average circulation for four separate years. This gives some idea of the variability that does appear to occur in the GAk. The bottom right panel also shows the location of three features that are important in future analyses. There is always a local maximum in dynamic height near position C. Though the exact location varies, the value of dynamic height at that maximum is taken as indicative of the California Gyre. Similarly, there is always a local minimum near position G. Again, the position does vary somewhat, but the minimum dynamic height near location G is chosen as descriptive of the GAk. Position B is also not really a specific location. In all maps there is a dividing line in the dynamic height field separating water in the NPC that ultimately reaches the coast of North America and heads northwards from that which heads southwards into the CCurr system. That dividing streamline is identified on each of the maps in Fig. 3, and that line must be identified by its behaviour close to the coast. Thus position B is the rough location where the dividing streamline meets the continental slope off North America.

We will use the dynamic height difference between G and C to represent the incoming flow in the NPC (ΔD_{NPC}). The difference between G and B is taken to represent the strength of surface flow in the Alaska Gyre (ΔD_{GAk}) and the difference between B and C is taken to represent the flow in the CCurr system (ΔD_{CCurr}).

Figure 4 shows each of these time series at monthly intervals, as well as the ratio, $f = \Delta D_{GAk}/\Delta D_{NPC}$, representing the fraction of NPC water that ultimately heads into the Alaska Gyre. As can be seen, on average 60% of the NPC water eventually flows into the GAk, with the remaining 40% flowing into the CCurr system. It is interesting that the variability in that fraction is not large, on only one occasion out of over 40 estimates is f observed to be less than 0.5 and has never yet been observed as large as 0.7. However, variability does occur and it is interesting to examine the patterns buried in the variability. At first glance there appears to be no obvious relationship among the various time series, that, as it turns out, is because there are two modes of variability that are occurring. The total flow of water in the NPC also shows relatively weak variability. One surprising result is that a Fourier analysis of each of the time series shows no evidence of any significant annual variability. The actual value of dynamic height at any one location in the north-east Pacific does show strong annual variability as one would expect, but the differences do not show significant annual cycles.

Let us take the three time series ΔD_{NPC}, ΔD_{GAk} and ΔD_{CCurr} in that order, remove the mean values and compute the covariance matrix. This matrix must be singular, since $\Delta D_{NPC} = \Delta D_{GAk} + \Delta D_{CCurr}$ and only two non-zero eigenvalues of the covariance matrix are found. The first two eigenvectors are as follows:
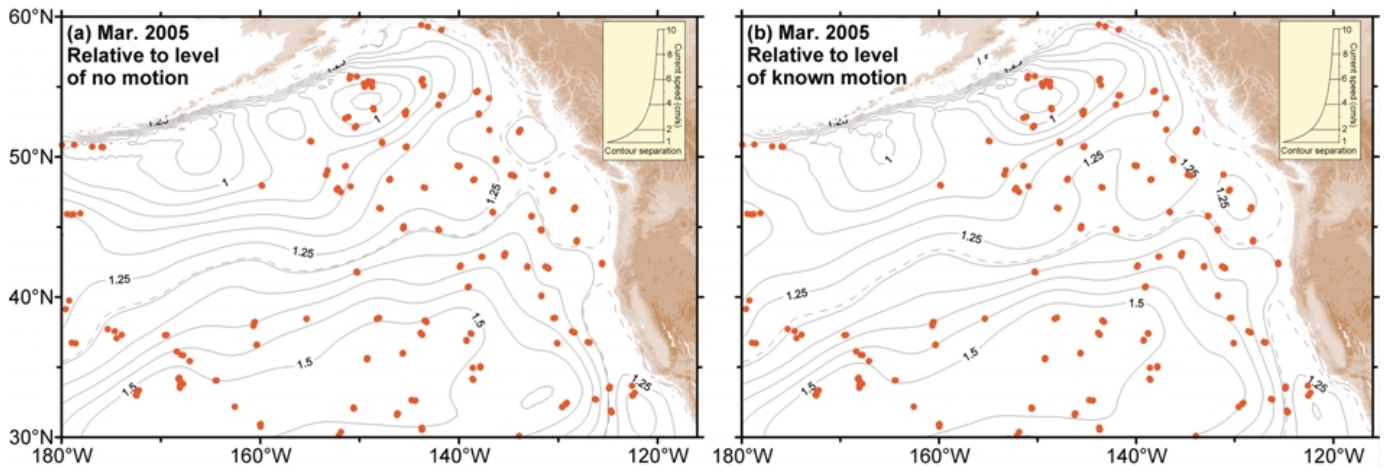
Fig. 2   The dynamic height at the surface of the north-east Pacific relative to (a) a level of no motion and (b) relative to a level of known motion.
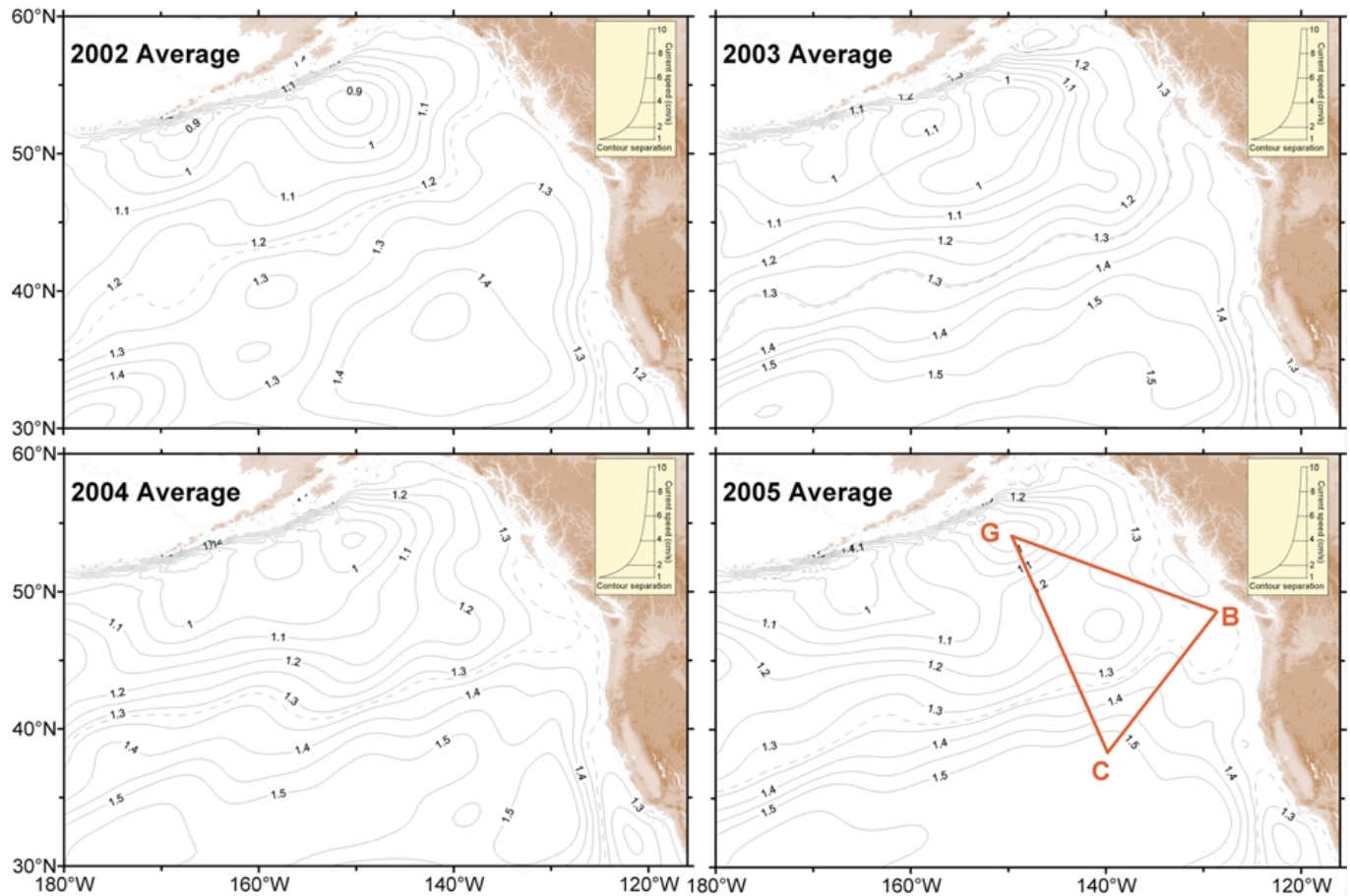

Fig. 3   The surface dynamic height fields averaged for 2002, 2003, 2004 and the first six months of 2005. The letters B, C and G identify three locations that are used in the paper. The scale at the top right indicates speeds associated with contour separations.

Mode 1: 82% of variance, vector is (0.807, 0.307, 0.505)
Mode 2: 18% of variance, vector is (0.113, 0.759, –0.642)

Mode 1 dominates and represents a simple "breathing mode" for the relationships among the current systems. When flow increases in the NPC, flow increases in both the GAk

and the CCurr system. Interestingly, the mean state has the majority of water flowing into the GAk, but the converse relationship occurs in the fluctuation field, so as the flow in the NPC increases, the fraction of water flowing into the GAk decreases. The second mode, accounting for 18% of the total variance, is the one that is related to the hypotheses of
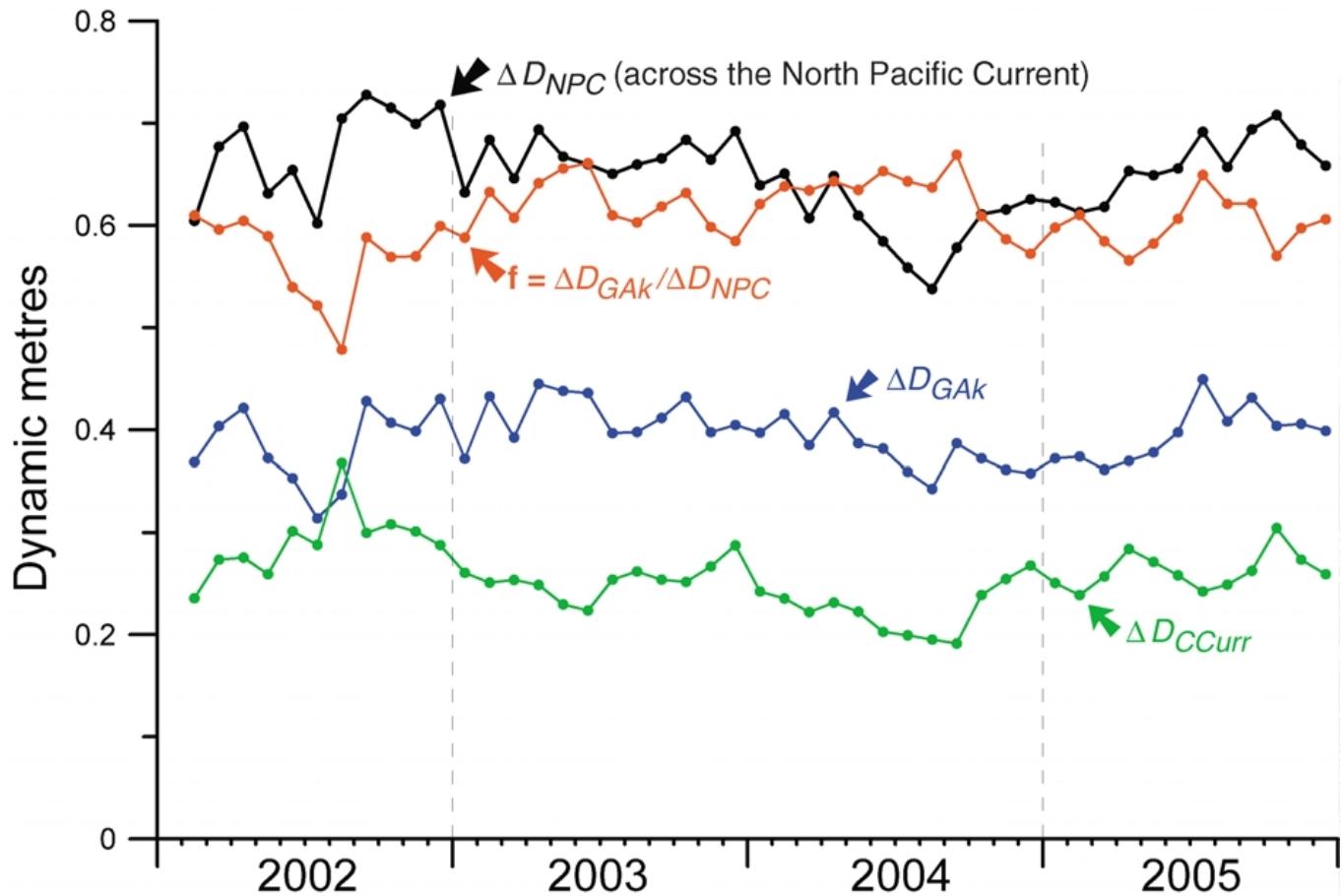
Fig. 4   Monthly values of the dynamic height differences across the NPC, CCurr and GAk, and in red, the fraction of NPC water flowing into the GAk.

Chelton and Davis (1982) and Hare et al. (1999), a bifurcation mode. The value of this mode for ΔD_{NPC} is essentially zero, so what it shows is, for no change in input waters a decrease of flow in the GAk is associated with an increase in the CCurr system.

Time series of the two modes are easily computed and are plotted in Fig. 5. As mentioned earlier in a different context, it is intriguing that there is no annual cycle apparent in either mode, this is verified by a Fourier transform. There is no evidence of any concentration of energy at the annual cycle, though a time series of dynamic height at a single point will show a strong annual cycle. The time series for EOF #1 suggests that there was an unusual event in the circulation of the GAk in summer and fall of 2004.

4 Discussion

Various authors have suggested that variability in the northeast Pacific might be dominated by some form of bifurcation mode. The concept being that even if the flow in the NPC is relatively stable the latitude of the bifurcation might change very substantially resulting in large changes in the distribution of water between the GAk and the CCurr. A previous paper by FC indeed does verify that the latitude of the bifurcation is highly variable, but it is seen here that this does not translate into large variability in fraction of the transports into the GAk and CCurr. A bifurcation mode certainly does exist, but variability in those current systems is not particularly large and the bifurcation mode itself accounts for only 36% of the total variance. It seems unlikely then that this effect is a significant contributor to variability in, for example, the supply of nutrients to the GAk.

Chelton and Davis (1982) examined this question using very different methods. In their paper they did not use observations in the GAk per se, rather they examined low-frequency sea-level variations from Mexico to the Aleutian Islands and computed EOFs describing the relationships between these coastal sea-level time series. With this method, only fluctuations can be examined as the mean circulation is wholly absorbed in the mean sea level. Their concept was that an increase in sea level in the GAk is in geostrophic balance with an *increase* in the circulation of the Gulf, however, an increase in sea level off California is balanced by a *decrease* in the circulation in the CCurr system. Thus, when they observed a dominant EOF that had constituted 38% of the total variance and had the same sign of amplitude at all sites from Baja, California to the Aleutians, they identified this as the bifurcation mode. However, in the current paper I find the leading mode accounting for 82% of the variance to be in a
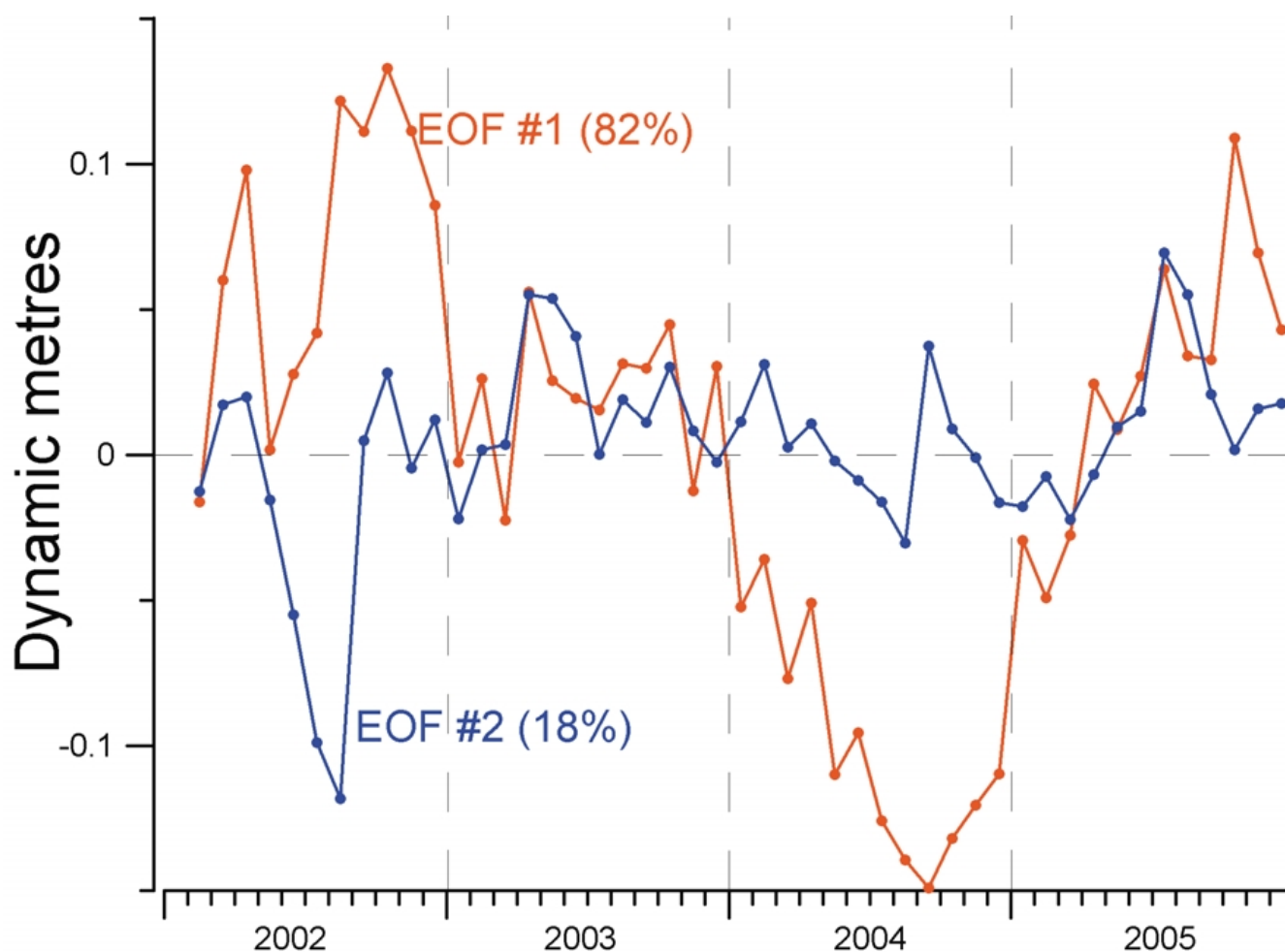
Fig. 5   Time series of the weights associated with the two non-trivial eigenvectors.

breathing mode, whereas Chelton and Davis reported no such mode. To explore this a little further I acquired sea levels for most of the stations used by Chelton and Davis in their 1982 paper. They had available sea levels up to and including 1975 whereas I now have access to a further 30 years of data. Some stations have been terminated since 1975 and I include only those stations used by Chelton and Davis that continue to operate today.

The anomalies of sea level height are plotted in Fig. 6 using the same style as the Chelton and Davis paper. Following the same analysis techniques I find a leading EOF which accounts for 27% of the total variance and with a structure to the first eigenvector as shown in Fig. 7. This does not appear to represent a mode which has a constant sign from Baja, California to the Aleutian Islands. The sites from San Diego to Prince Rupert do follow the pattern described by Chelton and Davis, but the sites northward of Prince Rupert appear to be completely unrelated to any variability at more southern locations. I conclude, therefore, that with 30 years extra data the results of Chelton and Davis can no longer be supported. A reviewer

has correctly pointed out that the Chelton and Davis mechanism implicitly assumes strong coupling between the gyre circulation and coastal sea levels. More recent studies have identified near-shore flows that affect coastal sea levels and which would tend to decouple the gyre from those signals.

Recent work by Douglass et al. (2006) has examined this same issue, but they used long expendable bathythermograph (XBT) sections and satellite altimetry. The data sources are substantially different and so it is not surprising that there are differences in results. The XBT lines have the advantage of very high resolution, but require some bold assumptions about the relationship between temperature and salinity before dynamic heights can be computed. Douglass et al. (2006) find the inverse relationship with about 65% of the NPC flowing into the CCurr system and 35% into the GAk. They also examine the variability and show evidence that both of the modes of variability identified in this paper (the so-called breathing mode and the bifurcating mode) are occurring, though they do not assign dominance to one or the other mode.
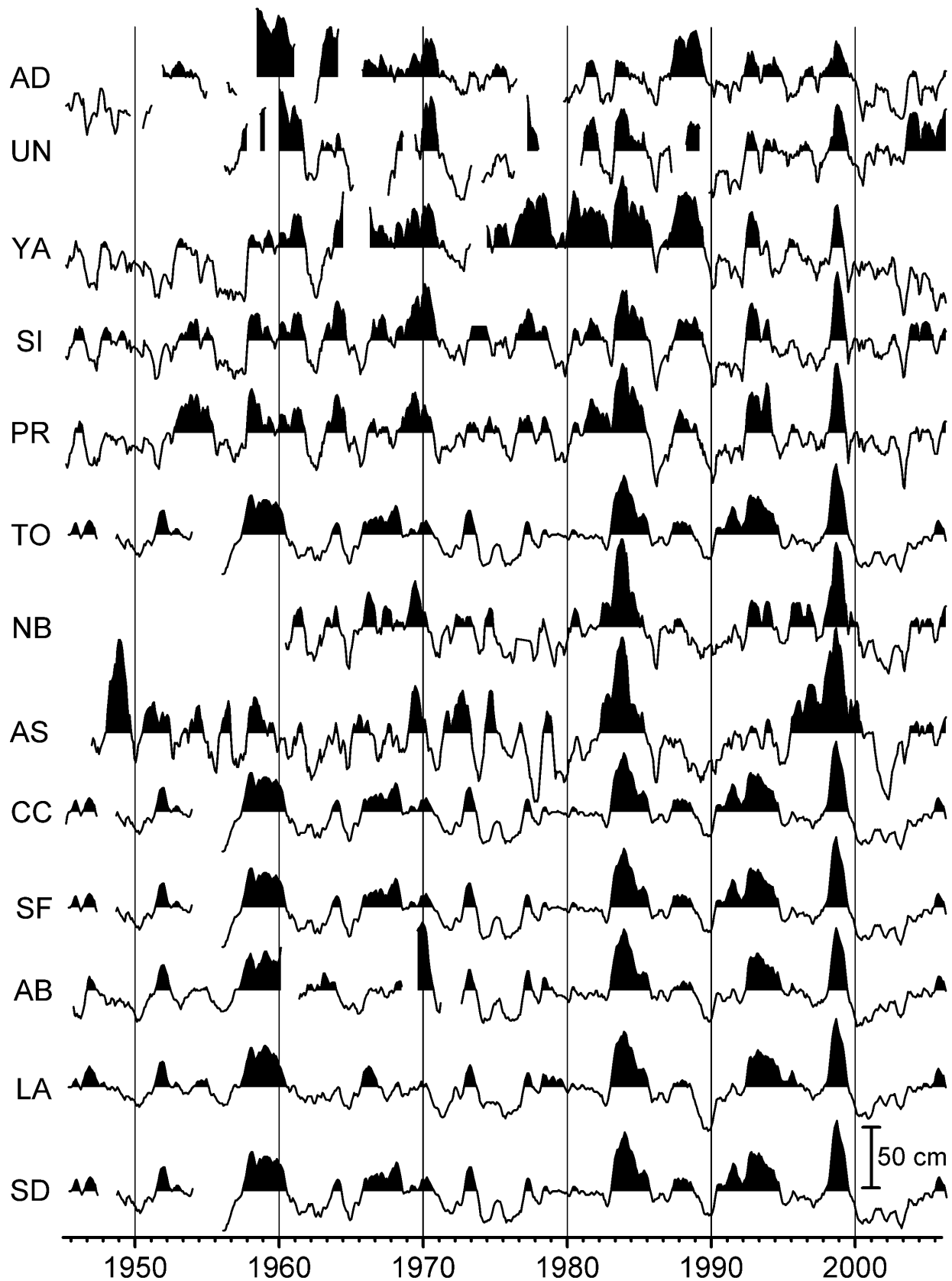
Fig. 6   The anomalies of sea level at stations around the CCurr and Alaska Gyre. The sites are as follows SD-San Diego, LA-Los Angeles, AB-Avila Beach, SF-San Francisco, CC-Crescent City, AS-Astoria, NB-Neah Bay, TO-Tofino, PR-Prince Rupert, SI-Sitka, YA-Yakutat, UN-Unalaska, AD-Adak. The bar at the bottom right shows a deviation of 50 cm.
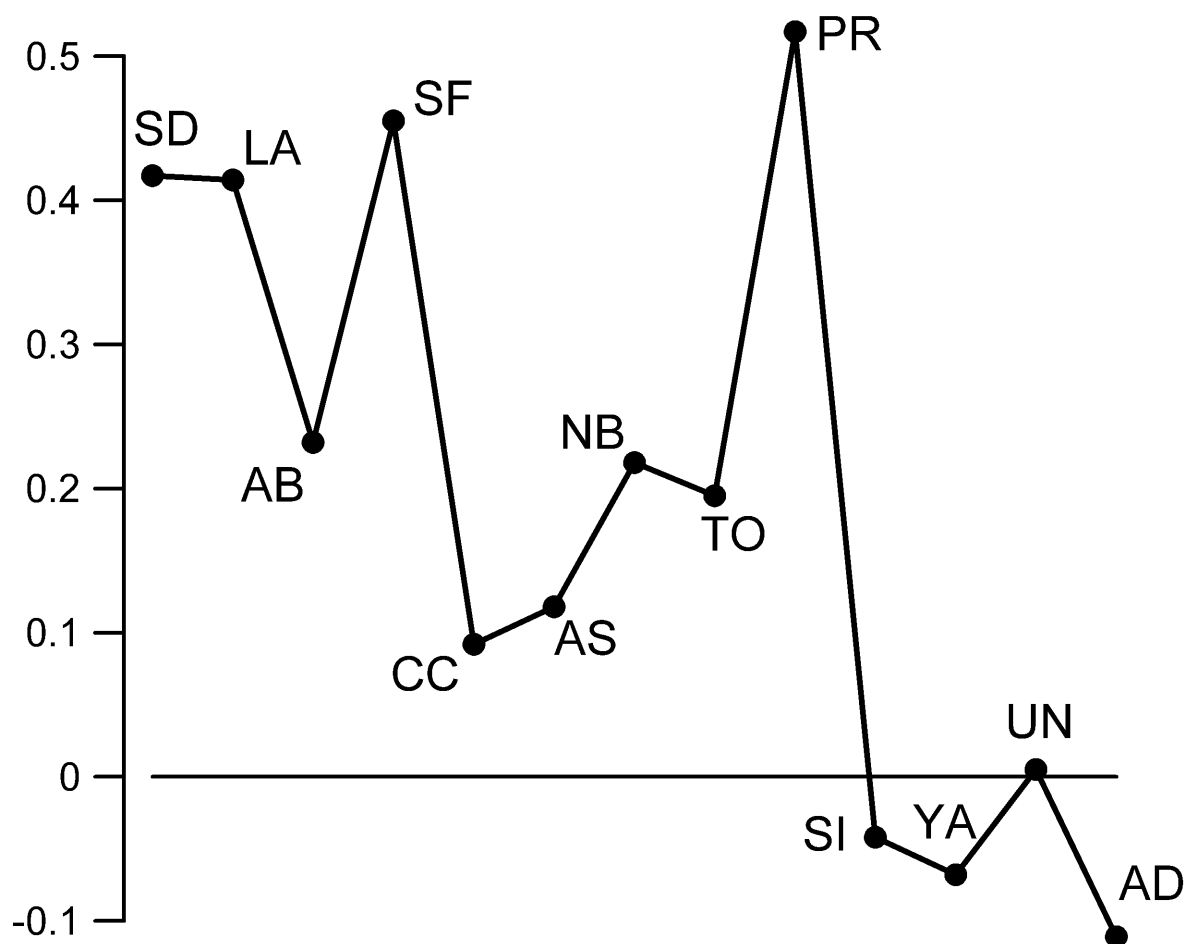
Fig. 7   The distribution of the (non-dimensional) weights in the leading EOF. Site names are as indicated in the caption for Fig. 6.

References

BOGRAD, S. J. and R. J. LYNN. 2003. Anomalous subarctic influence in the southern California Current during 2002. *Geophys. Res. Lett.* **30**: 8020, doi:10.1029/2003GL017446.

CHELTON, D. B. and R. E. DAVIS. 1982. Monthly mean sea-level variability along the west coast of North America. *J. Phys. Oceanogr.* **12**: 757–784.

CUMMINS, P.F. and G.S.E. LAGERLOEF. 2004. Wind-driven interannual variability over the northeast Pacific Ocean. *Deep Sea Res. 1*, **51**: 2105–2121.

DODIMEAD, A. J.; F. FAVORITE and T. HIRANO. 1963. Salmon of the North Pacific Ocean – Part II. Review of oceanography of the Subarctic Pacific Region. Int. N. Pac. Fish. Comm. Bull. No. 13, 195 pp.

DOE, L. A. E. 1955. Offshore waters of the Canadian Pacific Coast. *J. Fish. Res. Bd. Canada,* **12**(1): 1–34.

DOUGLASS, E.; D. ROEMMICH AND D. STAMMER, 2006. Interannual variability in northeast Pacific circulation. *J. Geophys. Res.* **111**: C04001, doi: 10.1029/2005JCO03015.

FRANCIS, R. C. and T. H. SIBLEY. 1991. Climate change and fisheries: what are the real issues? *NW Env. Journ.* **7**: 295–307.

FREELAND, H.J., G. GATIEN, A. HUYER and R.L. SMITH. 2003. A cold halocline in the northern California Current: an invasion of subarctic water. *Geophys. Res. Lett.* **30**: 1141, doi:10.1029/2002GL016663.

———. and P. CUMMINS. 2005. Argo: a new tool for environmental assessment and monitoring of the world's oceans. *Prog. Oceanogr.* **64**(1): 31–44

HARE, S.R.; N.J. MANTUA and R.C. FRANCIS. 1999. Inverse production regimes: Alaska and West Coast Pacific salmon. *Fisheries*, **24**: 6–14.

KOSRO, P. M. 2003. Enhanced southward flow over the Oregon shelf in 2002: A conduit for subarctic water. *Geophys. Res. Lett.* **30**: 8023, doi: 10.1029/2003GL017436.

MURPHREE, T. S.; J. BOGRAD, F. B. SCHWING and B. FORD. 2003. Large-scale atmosphere-ocean anomalies in the northeast Pacific during 2002. *Geophys. Res. Lett.* **30**: 8026, doi:10.1029/2003GL017303.

STRUB, P. T. and C. JAMES. 2003. Altimeter estimates of anomalous transports into the California Current during 2000–2002. *Geophys. Res. Lett.* **30**: 8025, doi:10.1029/2003GL017513.

THOMAS, A. C.; P. T. STRUB and P. BRICKLEY. 2003. Anomalous satellite-measured chlorophyll concentrations in the northern California Current in 2001–2002. *Geophys. Res. Lett.* **30**(15): 8022, doi:10:1029/2003 GL017409.

WHEELER, P. A.; A. HUYER and J. FLEISCHBEIN. 2003. Cold halocline, increased nutrients and higher productivity off Oregon in 2002. *Geophys. Res. Lett.* **30**: 8024, doi:10.1029/2003GL017395.

WICKETT, W. P. 1966. Ekman transport and zooplankton concentration in the North Pacific Ocean. *J. Fish. Res. Bd. Canada,* **24**(3): 581–594.